



# Hermite-cosh-Gaussian laser-induced third harmonic generation in plasma

Vinay Sharma<sup>1</sup> · Vishal Thakur<sup>1</sup> · Niti Kant<sup>1</sup>

Received: 29 November 2020 / Accepted: 20 April 2021 / Published online: 5 May 2021

© The Author(s), under exclusive licence to Springer Science+Business Media, LLC, part of Springer Nature 2021

## Abstract

Present work focuses on Hermite-cosh-Gaussian (HchG) laser-induced third harmonic generation (THG) in plasma on account of self-focusing. HchG laser beam gets self-focused due to ponderomotive force while propagating in plasma. Interaction of intense laser pulse results ponderomotive force on electrons and induce density perturbation that produces density oscillations at second harmonic frequency. Induced density perturbation beats with quiver velocity of electrons at laser frequency to produce a third harmonic nonlinear current. Application of wiggler magnetic field satisfies the phase matching condition which results resonant THG. Significant enhancement in the efficiency of THG is observed by using HchG laser profile for mode index  $m=2$ . Small variation in decentered parameter also affects the THG efficiency which shows the sensitivity of decentered parameter.

**Keywords** THG · Mode index · HchG · Self-focusing · Wiggler magnetic field · Plasma

## 1 Introduction

High intense laser propagates through the plasma resulting various interesting nonlinear phenomena which have been extensively studied by number of researchers in last few decades (Nakai and Takabe 1996; Corde et al. 2013; Hernandez et al. 2009; Zhang et al. 2017; Sointsev et al. 2011; Oagat et al. 2018). Due to interaction of intense laser beam with plasma medium the density perturbations occur and this result nonlinear change in refractive index of plasma medium. This gives rise to nonlinearity which has its important widespread applications such as inertial confinement fusion (Nakai and Takabe 1996), laser plasma accelerator (Corde et al. 2013), microscopic resonance imaging (Hernandez et al. 2009). The third harmonic generation is one of the most important nonlinear phenomena which was extensively studied by various researchers (Ganeev et al. 2010; Brandi 2009; Liu and Tripathi 2008; Tyagi 2016; Singh and Tripathi 2010; Kant et al. 2012). They observed that third harmonic generation takes place when intense laser beam propagates through plasma, created in a semiconductor. Wiggler magnetic field satisfy the resonance

---

✉ Niti Kant  
nitikant@yahoo.com

<sup>1</sup> Department of Physics, Lovely Professional University, G.T. Road, Phagwara, Punjab 144411, India

condition for higher efficiency of third harmonic pulse. Dhaiya et al. (2007) studied the Gaussian laser beam, where the resonance condition is satisfied by applying the density ripple and this results higher efficiency gain for second and third harmonics generated during laser plasma interaction. Resonant THG in cluster density was analysed by Vij et al. (2016). They observed that the presence of density ripples in clusters are responsible for the phase matching condition and this result increase in amplitude of harmonic generation takes place. Due to mismatch of group velocity of fundamental laser with that of the third harmonic pulse, the pulse slippage takes place. Thakur et al. (2016) had given the effect of density on the amplitude of third harmonic pulse, during laser plasma interaction. Shibhu et al. (1998) showed that density ripples in plasma are responsible for THG in a plasma channel and density perturbation satisfies the phase matching. Wiggler magnetic field was also used for resonant generation of third harmonic pulse (Rajput et al. 2009; Sharma et al. 2019).

Large number of researchers analyzed the properties of HchG laser using different approaches for self-focusing and harmonic generations. Nanda and Kant (2014) analyzed the HchG laser and presented the effect of density transition on self-focusing at optimum values of different laser parameters. Nanda et al. (2013a) studied the effect of density ramp on self-focusing for HchG laser beam for magneto-plasma, at different mode indices. Their study reveals that extraordinary mode is dominant over ordinary mode towards self-focusing. Wani and Kant (2016) studied the properties of HchG laser beam propagating through plasma under density transition. Plasma density ramp results stronger self-focusing and reduction in spot size is observed up to several Rayleigh lengths. Kaur et al. (2017) analyzed self-focusing for HchG laser by considering relativistic nonlinearity. Their study revealed that the self-focusing for different mode indices, at particular values of decentered parameter. Nanda et al. (2013b) studied the effect of decentered parameter on relativistic self-focusing of HchG laser beam in plasma and they reported the stronger self-focusing for mode index  $m=2$ . Patil et al. (2010) studied the HchG laser beam in collision less magneto plasma and they studied the effect of nonlinearity and spatial diffraction. Kant and Nanda (2014) had given the study of self-focusing of HchG laser in plasma and presented the effect of decentered parameter and frequency of incident laser on beam width parameter. Pathak et al. (2019) analyzed the properties of HchG laser beam, under density ripple, for different mode indices. Their study revealed that how the higher order terms affect the off-axial properties. Wadhwa and Singh (2019) analyzed the Hermite-Gaussian laser beam and studied the SHG and self-focusing in  $x$  and  $y$  direction at different mode indices and at various values of different laser parameters. Chib et al. (2020) studied the propagation properties for flattened Hermite-cosh-Gaussian light beam and they observed that Gaussian, cosh-Gaussian and Hermite cosh-Gaussian laser beam are the particular cases of their study. Chaudhary et al. (2020) reported the study of Hermite cosh-Gaussian laser beam propagating through hot electron, collisional and density modulated plasma and studied the effect of different laser parameters on tera hertz field emitted. Gavade et al. (2020) studied the self-focusing, considering elegant Hermite-cosh-Gaussian laser beam. They observed the role of decentered parameter for weaker relativistic and ponderomotive non-linearity. They observed stronger self-focusing with increasing values of decentered parameter. They observed the complex behaviour of beam width parameter at higher mode indices.

Hermite cosh-Gaussian beam is obtained by the superposition of two decentered Hermite-Gaussian beams as cosh-Gaussian ones (Belafhal and Ibnchaikh 2000). For  $m=0$  and  $b=0$ , the Hermite-cosh-Gaussian beams can be analyzed like Gaussian beam in nonlinear medium but the different values of mode index ( $m$ ) and decentered parameter ( $b$ ) are found to change the nature of self-focusing/defocusing of the beams significantly. In this study

we have analyzed the THG of a relativistic self-focusing HchG laser in plasma. Efficient THG is seen due to stronger self-focusing. Section 2 comprise the derivation of normalized amplitude for THG, results analysis is given in Sects. 3 and 4 contain the conclusion.

## 2 Theoretical formulation

Field distribution for Hermite cosh-Gaussian laser (Pathak et al. 2019) propagating through plasma is given as

$$\vec{E}_1 = A(x, y, z) \exp [i(\omega_1 t - k_1 z)] \tag{1}$$

$$\vec{B}_w = \hat{y} B_0 \exp(ik_0 z), \tag{2}$$

where  $\vec{k}_1$  is the wave number of incident laser pulse,  $\vec{B}_w$  is wiggler magnetic field and  $\vec{k}_0$  be the wiggler wave number,  $\omega_1$  be the angular frequency of incident laser and  $A$  be the amplitude of the incident laser pulse.

Electrons attain oscillatory velocity under the influence of ponderomotive force.

$$\vec{v}_1 = e \frac{\vec{E}_1}{m_0 \gamma i(\omega_1 + i\nu)} \tag{3}$$

where,  $m_0$  is the rest mass of the electron,  $\nu$  is the collision frequency of electrons and  $\gamma$  is the relativistic factor. Propagating laser exerts ponderomotive force on electrons and electrons attain an oscillatory velocity at  $2\omega_1$ . This oscillatory velocity combines with density ripple and produces perturbation in density at  $2\omega_1$ . This perturbation further beats with oscillatory velocity, at  $\omega_1$ , to produce third harmonic current density  $\vec{J}_3 = \vec{J}_3^L + \vec{J}_3^{NL}$ , where  $\vec{J}_3^L$  and  $\vec{J}_3^{NL}$  are given as (Kant et al. 2012)

$$\vec{J}_3^L = \frac{n_0 e^2 \vec{E}_3}{3m_0 \gamma i \omega_1}, \tag{4}$$

$$\vec{J}_3^{NL} = \frac{-n_0 e^5 B_w k_1 \vec{E}_1^3}{16ci\gamma^4 m_0^4 \omega_1^4 (\omega_1 + i\nu)} \left[ \frac{5k_1}{18\omega_1} + \frac{k_1 + k_0}{\omega_1 + i\nu} \right] \hat{x}. \tag{5}$$

The third harmonic field is

$$\nabla^2 \vec{E}_3 = \frac{4\pi}{c^2} \frac{\partial \vec{J}_3^L}{\partial t} + \frac{4\pi}{c^2} \frac{\partial \vec{J}_3^{NL}}{\partial t} + \frac{1}{c^2} \frac{\partial^2 \vec{E}_3}{\partial t^2}, \tag{6a}$$

where  $E_3 = A_3 e^{i(\omega t - kz)}$  and  $A_3 = A_{30}(r, z) e^{-ikS_{(r,z)}}$

$$A_{30}^2 = \frac{E_{30}^2}{f^2(z)} \left[ H_m \left( \frac{\sqrt{2}r}{r_0 f(z)} \right) \right]^2 e^{\left(\frac{b^2}{2}\right)} \left\{ \exp \left[ -2 \left( \frac{r}{r_0 f(z)} + \frac{b}{2} \right)^2 \right] + \exp \left[ -2 \left( \frac{r}{r_0 f(z)} - \frac{b}{2} \right)^2 \right] + 2 \exp \left[ - \left( \frac{2r^2}{r_0^2 f(z)^2} + \frac{b^2}{2} \right) \right] \right\} \tag{6b}$$

$H_m$  is the Hermite function and  $b$  is the decentered parameter.

Equations for beam width parameter (Vij et al. 2016) for different values of mode index ( $m$ ) are given as.

For  $m = 0$

$$\frac{\partial^2 f(z)}{\partial \xi^2} = \left[ 4 - 4b^2 - \frac{6E_0^2}{\gamma} \left( \frac{1}{m_0\gamma} \right) \left( \frac{\omega_1^2 r_0^2}{c^2} \right) \left( \frac{\omega_p^2}{\omega_1^2} \right) \exp \left( \frac{b^2}{2} \right) \right] \frac{1}{f^3(z)}$$

For  $m = 1$

$$\frac{\partial^2 f(z)}{\partial \xi^2} = \left[ 4 - 4b^2 - \frac{12E_0^2}{\gamma} \left( \frac{1}{m_0\gamma} \right) \left( \frac{\omega_1^2 r_0^2}{c^2} \right) \left( \frac{\omega_p^2}{\omega_1^2} \right) \exp \left( \frac{b^2}{2} \right) (b^2 - 2) \right] \frac{1}{f^3(z)}$$

For  $m = 2$

$$\frac{\partial^2 f(z)}{\partial \xi^2} = \left[ -8b^2 - \frac{24E_0^2}{\gamma} \left( \frac{1}{m_0\gamma} \right) \left( \frac{\omega_1^2 r_0^2}{c^2} \right) \left( \frac{\omega_p^2}{\omega_1^2} \right) \exp \left( \frac{b^2}{2} \right) (5 - 2b^2) \right] \frac{1}{f^3(z)}$$

where  $\alpha_1 = e^2 M / 6m_0^2 \gamma^2 \omega^2 k_b T_0$ , here, ' $M$ ' is the mass of the scatterer in the plasma, ' $k_b$ ' is the Boltzmann constant and ' $T_0$ ' is the equilibrium plasma temperature and  $\omega_p$  is the plasma frequency.

The particular integral of Eq. (6a) is as

$$\vec{E}_3 = A'_3 \exp [-i\{3\omega_1 t - (3k_1 + k_0)z\}] \tag{10}$$

$$A'_3 = A'_{30}(z)\psi_3 \text{ and } \psi_3 = \exp(-r^2/r_0^2 f_1^2) \exp(-3ik_1 s_1) \tag{11}$$

where,  $A_{30}$  is the constant, gives the amplitude of the pulse of THG.

With the help of Eqs. (10), (11) and (6a), we obtain

$$2\psi_3 \{i(3k_1 + k_0)\} \frac{\partial A'_{30}}{\partial \xi} + \left[ \left( \frac{9\omega_1^2 - 10\omega_p^2}{c^2} \right) + \frac{9\omega_1^2 \varphi(\vec{E}_1 \vec{E}_1^*)}{c^2} + \{i(3k_1 + k_0)\}^2 \right] A'_{30} \psi_3 + A'_{30} \frac{\partial^2 \psi_3}{\partial r^2} + A'_{30} \frac{\partial \psi_3}{r \partial r} = \frac{12\pi n_0 e^5 B_w k_1}{16c^2 m_0^4 \gamma^4 \omega_1^4} \left[ \frac{5k_1}{18\omega_1} + \frac{k_1 + k_0}{\omega_1 + iv} \right] \frac{\partial \vec{E}_1^3}{\partial t}, \tag{12}$$

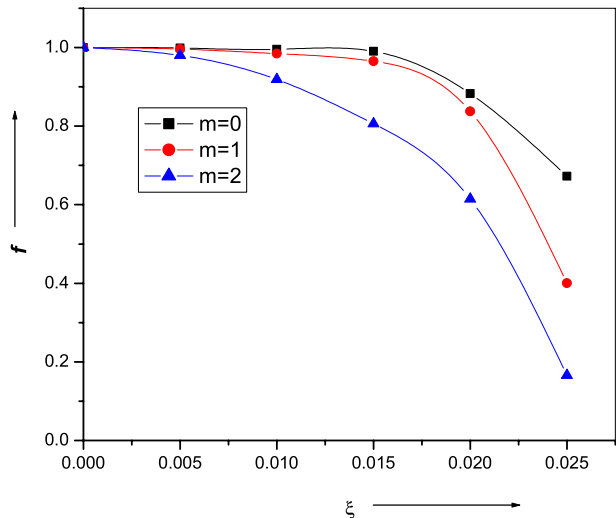
where,  $\xi = z/R_d$  is the normalized distance of propagation. After multiplying by  $\psi_3^* r dr$ , Eq. (12) is integrated with respect to  $r$ , we obtain

$$\begin{aligned}
 & 2i \frac{\partial A_{30}}{\partial \xi} \{2 - b^2\} + \left[ \begin{aligned} & -\left(\frac{9\omega_1^2 r_0^2}{c^2}\right) \left(1 - \frac{\omega_p^2}{9\omega_1^2}\right)^2 \{2 - b^2\} + A'_{30} \left\{ -\frac{24}{f^2(z)} \right\} \\ & + \left\{ -\frac{24}{2f^2(z)} + \frac{72b^2}{f^2(z)} - \frac{27b^4}{f^2(z)} - \frac{9b^2}{2f^2(z)} \exp(-2) - i\{2 - b^2\} \frac{\partial f_3}{f_3 \partial \xi} \right\} \\ & - \left[ \begin{aligned} & 10 \frac{\omega_p^2}{\omega_1^2} \left(\frac{\omega_1^2 r_0^2}{c^2}\right) - 9 \left(\frac{\omega_1^2 r_0^2}{c^2}\right) \\ & - 9 \left(\frac{\omega_1^2 r_0^2}{c^2}\right) \left(\frac{\omega_p^2}{\omega_1^2}\right) \frac{1}{\gamma} \left(1 - \exp\left[-\frac{3m_0 \gamma \alpha E_0^2}{4M}\right]\right) \end{aligned} \right] \{2 - b^2\} \end{aligned} \right] \\
 A_{30} = & \frac{3}{16\gamma^4} \left(\frac{\omega_p^2}{\omega_1^2}\right) \left(\frac{\omega_1^2 r_0^2}{c^2}\right) \left(1 - \frac{\omega_p^2}{\omega_1^2}\right)^{1/2} \left(\frac{e^2 A_{10}^2}{m_0^2 \omega_1^2 c^2}\right) \left(\frac{e B_w}{m_0 \omega_1 c}\right) \left[ \begin{aligned} & 3 \left(1 - \frac{\omega_p^2}{9\omega_1^2}\right)^{1/2} \\ & - \frac{31}{18} \left(1 - \frac{\omega_p^2}{\omega_1^2}\right)^{1/2} \end{aligned} \right] \{2 - 3b^2\} \tag{13}
 \end{aligned}$$

### 3 Result analysis

Equations (7), (8), and (9) are the derived expressions obtained for beam width parameter for different mode indices, whereas the expressions for normalized amplitude of third harmonic generation is given by Eq. (13). These coupled equations have been solved numerically for optimum values of different laser parameters as  $\omega_1 r_0/c = 27$ ,  $\omega_p/\omega_1 = 0.8$ ,  $\epsilon_2 A_{10}^2/\epsilon_0 = 1$ ,  $eA_{10}/m_0 \omega_1 c = 5$ , and  $eB_w/m_0 \omega_1 c = 3$ . The behaviour of beam width parameter ‘ $f$ ’ with  $\xi$  at  $m=0, 1$  and  $2$  respectively is depicted in Fig. 1. For  $m=0, 1$  and  $2$  we obtained the minimum value of the beam width parameter up to  $0.1$  for  $m=2$ . This shows that the self-focusing becomes stronger for  $m=2$ . When mode index is having

**Fig. 1** Behaviour of beam width parameter  $f$  of the pump laser with normalized propagation distance  $\xi$  for different values of  $m = 0, 1$  &  $2$ . The other parameters are  $\omega_1 r_0/c = 27$ ,  $\epsilon_2 A_{10}^2/\epsilon_0 = 1$ ,  $eA_{10}/m_0 \omega_1 c = 5$ ,  $eB_w/m_0 \omega_1 c = 3$  and  $\omega_p/\omega_1 = 0.8$



odd values then the beam profile becomes the sinusoidal curves modulated by a Gaussian envelope. Whereas, for even values of  $m$  the intensity distribution can be regarded as the cosine curves as the case of the cosh-Gaussian beams (Chaudhary et al. 2020) due to which self-focusing becomes stronger for  $m=2$ . Patil et al. (2008) shows the similar behaviour of HchG laser beam and their study outcome showed that for  $m=2$  the self-focusing increases.

The graphical analysis of normalized amplitude of third harmonic pulse with normalized distance  $\xi$ , at different values of normalized intensity is shown in Fig. 2, where other parameters are same as in Fig. 1. We obtain the values of normalized amplitude in THG as 0.035, 0.24 0.525 for different values of normalized intensity. With increase in intensity of fundamental laser the ponderomotive force becomes stronger and due to higher oscillatory velocity of electrons the stronger self-focusing is observed.

Figure 3 shows the graphical study of the variation of normalized amplitude in THG with  $\xi$  for optimum values of normalized wiggler magnetic field and varying the intensity of fundamental laser. It is quite clear from the graph that the normalized amplitude of THG increases with increase in normalized wiggler field. Sharma et al. (2013) studied the THG for Gaussian laser pulse under the effect of wiggler magnetic field and they observed that gain is significant on increasing wiggler magnetic field. The peak value of normalized amplitude for third harmonic pulse is 0.132, where as in present work, for HchG laser beam the peak value of normalized amplitude is nearly 0.54. This shows that gain is more prominent when we use the Hermite-cosh-Gaussian laser profile. Figure 4 gives the graphical variation of normalized amplitude of THG with linear propagation distance, at different values of normalized plasma density  $\omega_p/\omega_1$ . We observed that the normalized amplitude of THG attains its peak values as 0.14, 0.37 and 0.55 at  $\omega_p/\omega_1=0.4, 0.6$  &  $0.8$  respectively. With increase in plasma density the phase velocity of pulse decreases, results increase in refractive index due to which gain in efficiency increases. Figure 5 shows the variation of  $A_{30}/A_{10}$  with linear propagation distance, at

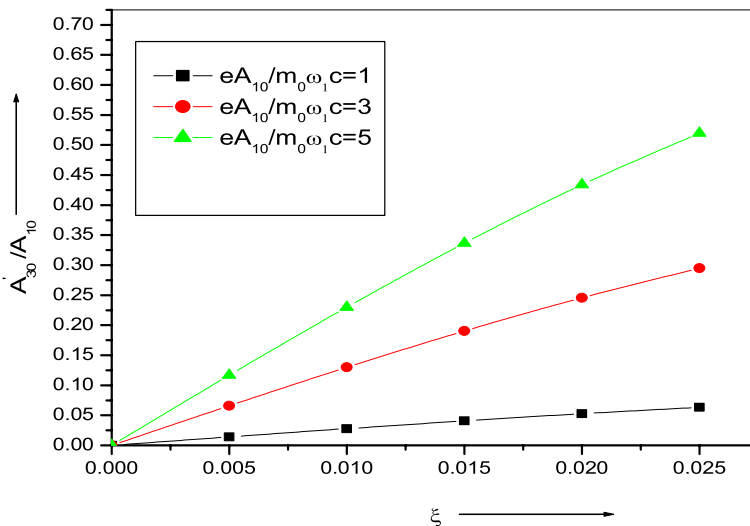


**Fig. 2** Variation of  $A'_{30}/A_{10}$  with  $\xi$  for different values of  $eA_{10}/m_0\omega_1c = 1, 3$  &  $5$ . The other parameters can be same as in Fig. 1

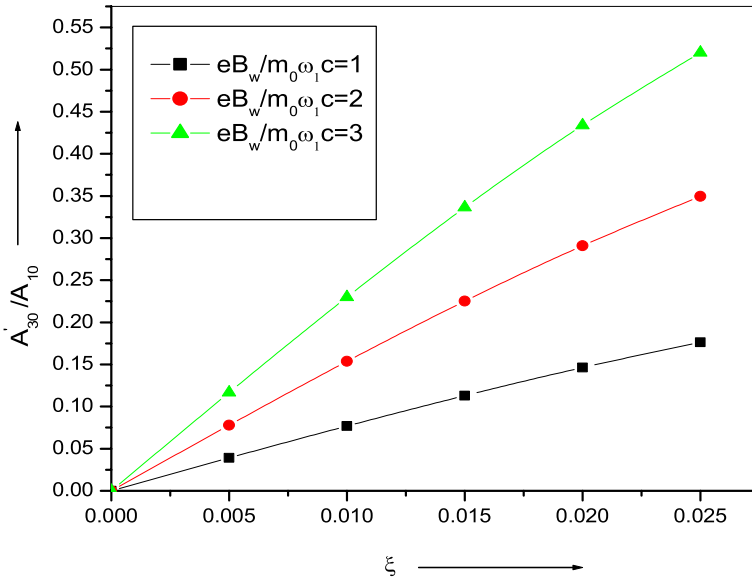


**Fig. 3** Behaviour of  $A'_{30}/A_{10}$  with  $\xi$  for different values of  $eB_w/m_0\omega_1c = 1, 2 \& 3$

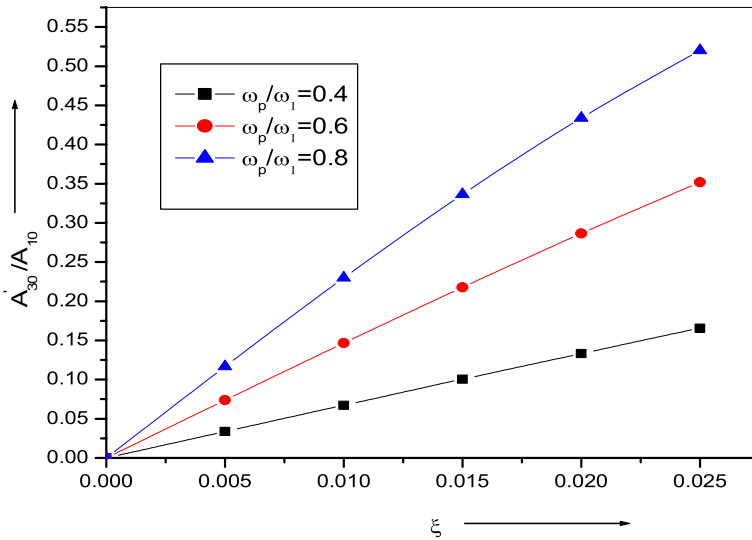


**Fig. 4** Behaviour of  $A'_{30}/A_{10}$  with  $\xi$  for different values of  $\omega_p/\omega_1 = 0.4, 0.6 \& 0.8$

different values of decentered parameter taken as  $b = 0.52, 0.54 \& 0.56$ . It is observed that the small variation of decentered parameter results changes in normalized amplitude, thus showing the sensitivity of decentered parameter. The sensitivity of decentered parameter was given by Nanda et al. (2013b) for HchG laser beam in magneto-plasma.

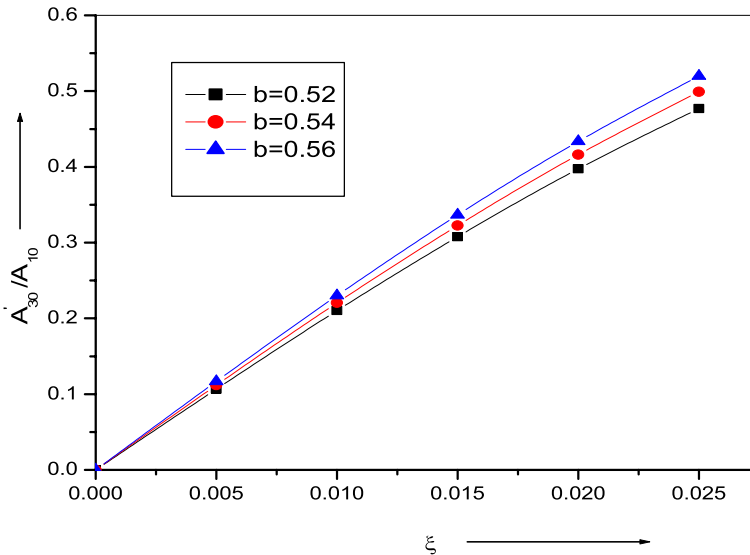


**Fig. 5** Behaviour of  $A'_{30}/A_{10}$  with  $\xi$  for different values of  $b = 0.52, 0.54$  &  $0.56$

## 4 Conclusion

The outcome of study shows stronger self focusing is stronger at higher values of mode index and attain its value up to 0.1 for  $m=2$ . Stronger ponderomotive force results higher quiver velocity, which is responsible for change in dielectric properties of plasma medium. Sharp increase in the amplitude of third harmonic pulse is observed for  $m=2$  for increasing values of intensity of laser propagating through plasma, normalized wiggler magnetic field and normalized plasma density. It is necessary to mention that efficiency gain is higher in case of HchG laser beam as compared to Gaussian laser beam. The small variation of decentered parameter ( $b$ ) shows the sensitivity of  $b$  on THG.

**Acknowledgement** This work is supported by the TARE Scheme (Grant No. TAR/2018/000916) of SERB, DST, New Delhi, India.

## References

- Belafhal, A., Ibnchaikh, M.: Propagation properties of Hermite-cosh-Gaussian laser beams. *Opt. Commun.* **186**, 269–276 (2000)
- Brandi, H.S.: Third-harmonic generation via laser-plasma interaction: Beyond the low-density approximation. *J. Mod. Opt.* **45**, 573–585 (2009)
- Chaudhary, S., Manendra, K.P., Singh, U. Verma., Malik, A.K.: Radially polarized terahertz (THz) generation by frequency difference of Hermite Cosh Gaussian lasers in hot electron-collisional plasma. *Opt. Lasers Eng.* **134**, 106257 (2020)
- Chib, S., Essakali, L.D., Belafhal, A.: Propagation properties of a novel generalized flattened Hermite-cosh-Gaussian light beam. *Opt. Quantum Electron.* **52**, 277 (2020)
- Corde, S., Phuoc, K.T., Lambert, G., Fitour, R., Malka, V., Rousse, A.: Femto second X rays from laser-plasma accelerators. *Rev. Mod. Phys.* **85**, 1–48 (2013)
- Dahiya, D., Sajal, V., Sharma, A.K.: Phase-matched second and third harmonic generation in plasma with density ripple. *Phys. Plasmas* **14**, 123104 (2007)
- Ganeev, R.A., Boltaev, G.S., Tugushev, R.I., Usmanov, T., Baba, M., Kuroda, H.: Third harmonic generation in plasma plumes using picosecond and femtosecond laser pulses. *J. Opt.* **12**, 055202 (2010)



- Gavade, K.M., Urunkar, T.U., Vhanmore, B.D., Valkunde, A.T., Takale, M.V., Patil, S.D.: self-focusing of Hermite cosh Gaussian laser beams in a plasma under a weakly relativistic and ponderomotive regime. *J. Appl. Spectrosc.* **87**, 499–504 (2020)
- Hernandez, C.F., Ortiz, G.R., Tseng, S.Y., Gaja, M.P., Kippelen, B.: Third-harmonic generation and its applications in optical image Processing. *J. Mater. Chem.* **19**, 7394–7401 (2009)
- Kant, N., Nanda, V.: Stronger self-focusing of Hermite-Cosh-Gaussian (HChG) laser beam in plasma. *OA. Lib J.* **1**, 2333 (2014)
- Kant, N., Gupta, D.N., Suk, H.: resonant third harmonic generation of a short pulse laser from electron hole plasmas. *Phys. Plasmas* **19**, 013101 (2012)
- Kaur, S., Kaur, M., Kaur, R., Gill, T.S.: Propagation characteristics of Hermite-cosh-Gaussian laser beam in a rippled density plasma. *Laser Part Beams* **35**, 100–107 (2017)
- Liu, C.S., Tripathi, V.K.: Third harmonic generation of a short pulse laser in a plasma density ripple created by a machining beam. *Phys. Plasmas* **15**, 4 (2008)
- Nakai, S., Takabe, H.: Principles of inertial confinement fusion physics of implosion and the concept of inertial fusion energy. *Rep. Prog. Phys.* **59**, 1071–1131 (1996)
- Nanda, V., Kant, N.: Strong self-focusing of a cosh-Gaussian laser beam in collisionless magneto-plasma under plasma density ramp. *Phys. Plasmas* **21**, 72111 (2014)
- Nanda, V., Kant, N., Wani, M.A.: Self-focusing of a Hermite-cosh-Gaussian laser beam in a magneto-plasma with ramp density profile. *Phys. PlasmaS* **20**, 113109 (2013a)
- Nanda, V., Kant, N., Wani, M.A.: Sensitiveness of decentered parameter for relativistic self-focusing of Hermite-cosh-Gaussian laser beam in plasma. *IEEE Trans. Plasma Sci.* **41**, 2251–2256 (2013b)
- Oogat, Y., Votobyyev, A., Guo, C.: Optical third harmonic generation using nickel nanostructure-covered micro-cube structures. *Materials* **11**, 501–506 (2018)
- Pathak, N., Kaur, M., Gill, T.S.: Non-paraxial theory of self-focusing/ defocusing of Hermite cosh Gaussian laser beam in ripple density plasmas. *Contrib. Plasma Phys.* **26**, 1–14 (2019)
- Patil, S.D., Takale, M.V., Dongare, M.B.: Propagation of Hermite-cosh-Gaussian laser beams in n-InSb. *Opt. Commun.* **281**, 4776–4779 (2008)
- Patil, S.D., Takale, M.V., Navare, S.T., Dongare, M.B.: Focusing of Hermite-cosh-Gaussian laser beams in collisionless magnetoplasma. *Laser Part Beams* **28**, 343–349 (2010)
- Rajput, J., Kant, N., Singh, H., Nanda, V.: Resonant third harmonic generation of a short pulse laser in plasma by applying a wiggler magnetic field. *Opt. Commun.* **282**, 4614–4617 (2009)
- Sharma, H., Jaloree, H., Prashar, J.: Magnetic field wiggler assisted third harmonic generation of a Gaussian laser pulse in plasma. *Turk. J. Phys.* **37**, 368–374 (2013)
- Sharma, V., Thakur, V., Kant, N.: Third harmonic generation of a relativistic self-focusing laser in plasma in the presence of wiggler magnetic field. *High Energy Dens. Phys.* **32**, 51–55 (2019)
- Shibu, S., Tripathi, V.K.: Phase-matched third harmonic generation of laser radiation in a plasma channel: non-local effects. *Phys. Lett. A* **239**, 99–102 (1998)
- Singh, R., Tripathi, V.K.: Brillouin shifted third harmonic generation of a laser in a plasma. *J. Appl. Phys.* **107**, 113308 (2010)
- Sointsev, S., Sukhorukov, A., Neshev, D.N., Iliev, R.: Cascaded third harmonic generation in lithium niobate nanowaveguides. *Appl. Phys. Lett.* **98**, 23 (2011)
- Thakur, V., Kant, N.: Effect of pulse slippage on density transition-based resonant third harmonic generation of short pulse laser in plasma. *Front. Phys.* **11**, 115202 (2016)
- Tyagi, Y.: Bernstein wave aided laser third harmonic generation in a plasma. *Phys. Plasmas* **23**(093115), 1–5 (2016)
- Vij, S., Kant, N., Aggarwal, M.: Resonant third harmonic generation in clusters with density laser: effect of pulse slippage. *Laser Part Beams* **34**, 171–177 (2016)
- Wadhwa, J., Singh, A.: Generation of second harmonics by a self-focused Hermite-Gaussian laser beam in collisionless plasma. *Phys. Plasmas* **26**, 062118 (2019)
- Wani, M.A., Kant, Niti: Self-focusing of Hermite-cosh-Gaussian (HChG) laser beams in plasma under density transition. *Adv. Opt. Photon.* **2014**, 1–6 (2016)
- Zhang, Z., Kuzmin, N.V., Groot, M.L., Munck, J.C.D.: Extracting morphologies from third harmonic generation images of structurally normal human brain tissue. *BMC Bioinf.* **33**, 1712–1720 (2017)